Graduate School of Frontier Sciences, The University of Tokyo

Natural Environmental Studies, Division of Environmental Studies

Natural Environmental Changes

School Year 2019 Master Thesis

Large Scale High Resolution Geomorphological Monitoring of Beach-Dune System by UAV SfM on Kujukuri and Uchinada Beaches

九十九里浜および内灘海岸における UAV-SfM を用いた砂浜-砂丘系の広範囲高解像度地形モニタリング

Submission: July 19, 2019
for completion in September 2019

Supervisor: Professor Toshihiko Sugai

47-176809 Kungaa Mergen

Contents

1 Introduction

1.1 Background

Over the years, coastal science has accumulated a variety of methods for monitoring coastal areas (Sutherland, 2007). But in recent years, structure from motion (SfM) photogrammetry became a powerful and very popular tool in the hands of researchers. Digital coastal imagery from unmanned aerial vehicles (UAVs) combined with structure-from-motion (SfM) photogrammetry and modern per-pixel image matching algorithms could provide us a time-series of digital elevation models in an automated and inexpensive way. But it is worth noting that most of researches are conducted in limited areas (Casella, et al., 2016) (Medjkane, et al., 2018) (Westoby, et al., 2018) (Mancini, et al., 2013). While researches on a larger scale are less common and are just beginning to gain popularity (Laporte-Fauret, et al., 2019). Of course, the scale of the study should depend on the tasks, but in the case of monitoring the scale should be important.

For methodological purposes it was important to take a stretch of shore that would be a separate morpho- and lithodynamic unit. I believe that choosing small plot of area will increase the impact of research bias and capturing dynamic of only part of the unit, leaving us without a complete picture at least within unit.

1.2 Objectives of Research

First of all, we took into account our possibilities. There are a lot of commercial solutions, which could cover bigger areas and provide better accuracy, both in multi-rotor or fixed-wing embodiment (Boon, Drijfhout, & Tesfamichael, 2017). But purchasing some additional equipment without fully understanding the processes themselves would be an unwise decision. So, we relied on equipment, which already were available in the laboratory of Natural Environmental Changes – small consumer class UAV and low-cost RTK GNSS.

Based on such initial conditions, we tried to take advantage of our equipment. In this way, we developed a low-cost and replicable UAV photogrammetry workflow to monitor the morphological evolution of beach-dune systems in a large scale. At the same time, the main goal was still achieving greater insight into beach-dune dynamics across large area at high resolution.

1.3 Study Site

Because of monitoring task, during which I will have to visit study area several times, I have decided to concentrate on Pacific Ocean side of Japan. Due to accessibility from Kashiwa campus of Tokyo University, and relatively less urbanization of the area, I have opted for Kujūkuri Beach in Chiba Prefecture will be best option for me in case of research methods processing and long-term monitoring (Figure 1).

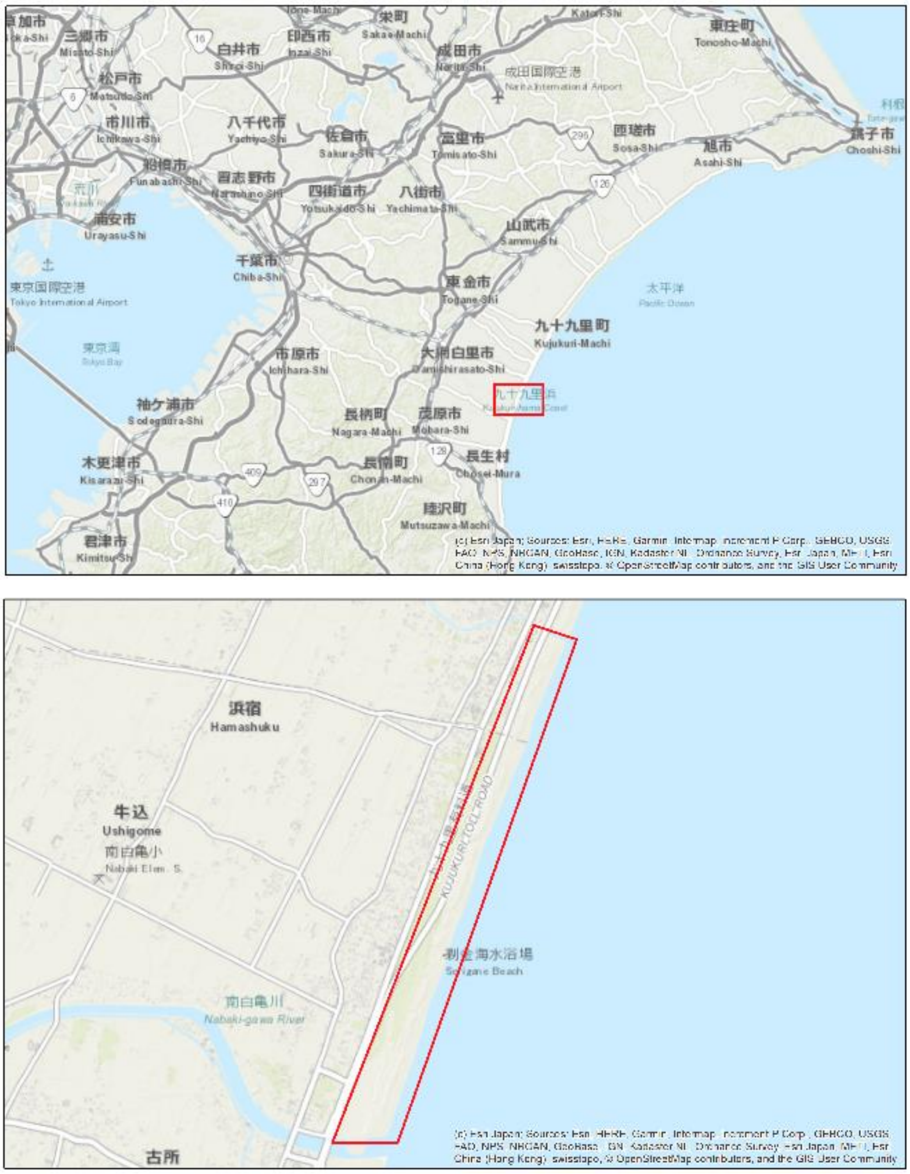

Figure 1 Map of study area on Kujukuri beach

Another factor that prompted to choose this area was the fact that in 2015 site between Nabaki and Magame rivers on Kujukuri beach was surveyed by Shoichiro Uchiyama, graduate of Natural Environmental Changes laboratory, using UAV carrying a mirrorless digital camera. Unfortunately, later it turned out that the data were collected in 2 stages with a difference of a week between which a storm event occurred, also it was not possible to perform a georeferencing of acceptable quality and control accuracy of DSM. Though we failed to use this data, I found it important to mention this fact about choosing study area.

For methodological purposes it was important to take a stretch of shore that would be a separate morpho- and lithodynamic unit. I believe that choosing small plot of area will increase the impact of research bias and capturing dynamic of only part of the unit, leaving us without a complete picture at least within unit.

So, in 11-13th of February 2018, we surveyed the 3250-meter long area between Nabakigawa and Horikawa rivers, which forms separate unit on the Kujukuri beach, Chiba Prefecture (Figure 1). Aerial photography area is ~1.3 sq. km. After survey was repeated 3 times, in 30th of June, 15th of September and 8th of February 2019.

Also, in 2018, during the field practice of the Natural Environmental Changes laboratory, it became possible to obtain data on the coast of the Japanese Sea, in Ishikawa Prefecture.

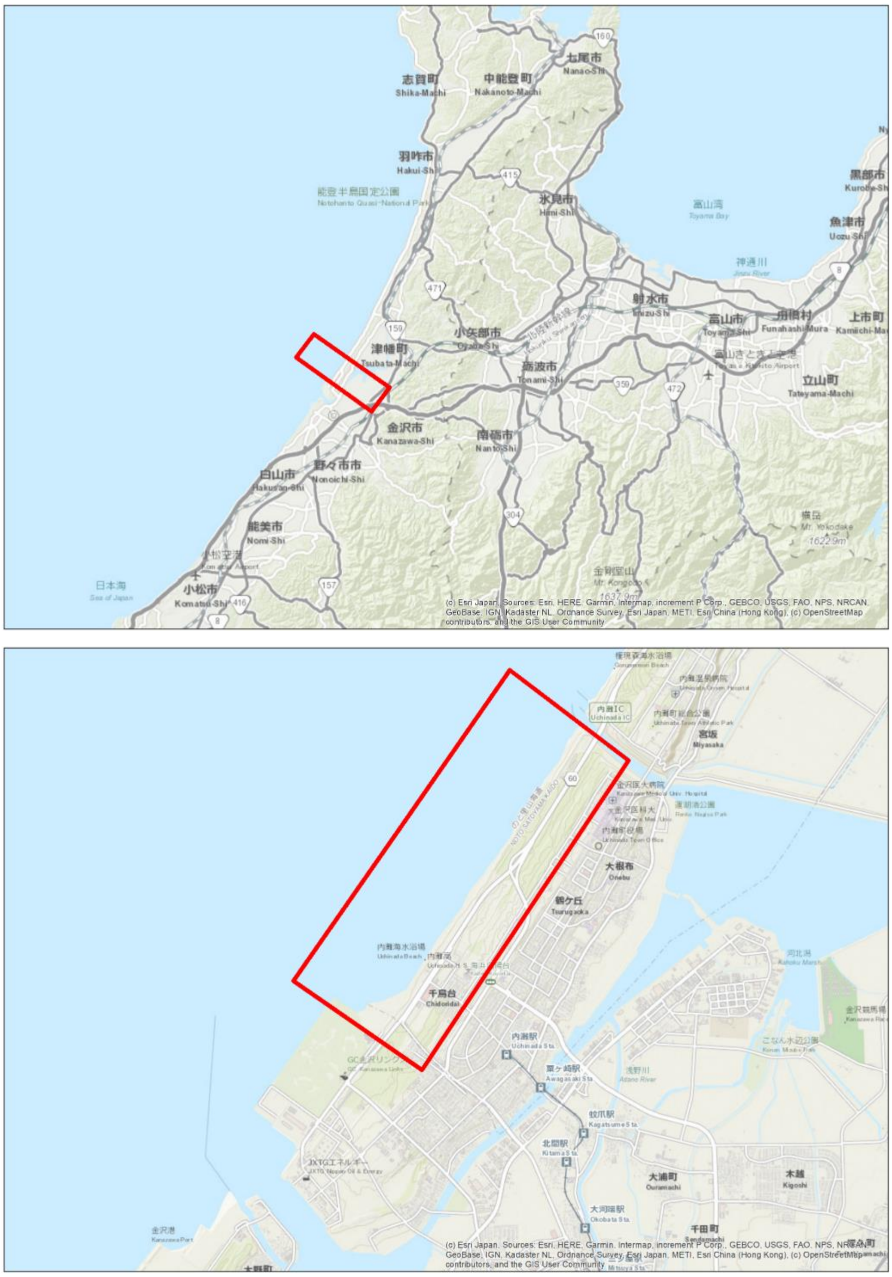

Figure 2 Map of study area on Uchinada beach

We have chosen area of the coast with similar length as Kujukuri beach, which also would be separate morpho- and lithodynamic unit. In case of Ishikawa prefecture, we surveyed 3870-meter stretch beach in Uchinada-machi (Figure 2). From the north it is limited by Morishita river, from the south – by groyne. Survey was conducted 2 times – 2nd of September in 2018 and 8th of March 2019.

2 Methodology

2.1 Mission Planning

To be more efficient during survey we were using combination of 2 apps:

•DJIFlightPlanner for Windows OS (www.djiflightplanner.com)

•Litchi app for Android OS or iOS (flylitchi.com)

DJIFLightPlanner was used to build mission grid and allowed us to control critical imaging parameters: flying height, flight speed, forward overlap, side overlap, ground distance sample & imaging frame rate. Controlling those parameters provides complete control over photogrammetric aerial survey mission. In case of Kujukuri beach, we usually set 80% front and side overlap from a height of 60 meters to achieve ground sample distance (GSD) ~2,5 cm for orthomosaic. On Uchinada beach due to time limits we decided to do bigger ground sample distance (~4 cm per pixel) for orthomosaic and fly higher (~90 m).

After building in DJIFligthPlanner. the mission is exported in csv format and imported into "Mission Hub" of Litchi app. This application allowed us to fly in autopilot mode so to be more efficient during field works. Basically, manual flight is more time-consuming and labor-intensive. In addition, proper control of critical imaging parameters merely impossible.

Initially, we tried to get both combination of nadir and oblique photos of surface. Although some studies (Vacca, Dessì, & Sacco, 2017) prove the superiority of this method, especially in urban areas, in case of beach-dune systems turn out to be unnecessary – adding oblique aerial photos did not improve accuracy in our case, but made it more laborious.

During first survey we took 3124 aerial photos by using small consumer class UAV (DJI Phantom 3 Standard) with 12 mpx camera. Unfortunately, we had to perform more than 13 flights (including flights for oblique shooting and failed flights due to technical issues) and it take 3 day of work of half a dozen people. Further, I decided to reduce the number of polygons (respectively, the number of flights) up to 5 and the number of aerial photos decreased to ~2500 photos due to optimization. Goal for both Chiba and Ishikawa prefectures were 1 day of work and ultimately, we achieved this goal.

2.2 High Accuracy Georeferencing

Previously solutions for proper UAV SfM workflows were restricted by the requirement for ground control gained with costly gear. So sometimes researchers relied on direct georeferencing - work process that ignores ground control and uses just the camera positions to georeference the SfM results (Carbonneau & Dietrich, 2017). While, accuracy of such kind of workflow might be enough for some types of research, to achieve decimeter accuracy it was necessary to use real-time kinematic (RTK) GNSS. Basically, ground control is required to georeference, refine the camera alignment parameters, and remove any artefacts and irregularities of camera distortion from the topographic model.

Fortunately, in recent years, not only has the quality of consumer drones improved, allowing them to be used for research, but low-cost RTK GNSS solutions appeared. Even more, there is possibility to use smartphones built-in GNSS as an RTK solution (Robustelli, Baiocchi, & Pugliano, 2019), although accuracy of such solution still far from using as research equipment.

In our case we used low-cost Emlid Reach GNSS. Emlid Reach can provide cm accuracy during static tests and cm precision during static and kinematic tests for post-processed solutions (Erikkson, 2016).

Number of ground-control points were another problem. While it obviously should be more than 3, but it is also obvious that impossible to increase their number indefinitely. Based on other studies ((Oniga, Breaban, & Statescu, 2018) and (Tonkin & Midgley, 2016)), it became clear that 5 is a magic number on which accuracy would be sufficient and further increase of GCP number would not increase accuracy drastically.

So, we placed ground control points (GCPs) in way that they fall on the 4 corners and center of each polygon. There were also 2 check points (CPs) at each polygon placed among GCPs. GCPs and CPs coordinates were determined by low-cost post-processing kinematic (PPK) Emlid Reach GNSS.

2.3 Data Collection

As I mentioned above – goal was achieving 1-day workflow for both survey areas. The most important point to achieve for this goal was the separation of tasks. In the end, we have achieved that 3 people are enough to complete the tasks:

1. Person for GCPs and CPs placement and helping with georeferencing
2. Person for georeferencing
3. Drone operator

To coordinate the work, we again used couple applications:

- Maps.me (maps.me) – free navigation software for both Android OS and iOS. We uploaded kml files with GCPs and CPs, so that everyone knows their location. Well, you can replace it with any other navigation application, which supports importing file with GCPs and CPs. In our case, it was the optimal solution.
- Zello (zello.com) - the push-to-talk mobile app that simulates walkie talkie. Works wherever 3G or 4G mobile communication possible, which usually provides much better coverage than consumer walkie-talkie (less than 1 km range in good conditions). Although it is possible to exchange information in different messenging apps, concept of walkie-talkie much more suitable for field work, where several people participate.

In place of the usual process is as follows:

1. 1st person goes to arrange all GCPs and CPs.
2. The rest first go to install base station for RTK GNSS.

3. After installation 2nd person prepares RTK GNSS Rover, and together with the drone operator go to the place where 1st person began to arrange GCPs and CPs.
4. The 2nd person successively begins to take the coordinates of GCPs and CPs.
5. Drone operator should fly as soon as arrangement of GCPs and CPs of each corresponding polygon ends.
6. Usually, 1st person ends earlier, so he will usually help with georeferencing.

Parallelizing processes allows to be highly efficient as a team, but it should be noted that 2nd person and drone operator must be trained and know how to trouble-shoot problems with RTK GNSS and UAV, respectively.

2.4 Structure from Motion Processing

UAV images were processed through the SfM workflow in Agisoft Metashape (previously known as Photoscan), available from the Russian software development company AgiSoft LLC. Metashape generates 3D spatial data to be used in GIS applications. The data were processed according to the following scheme:

1. Import images
2. Align images
3. Set markers on GCPs (Ground control points) and import coordinates
4. Build Dense Cloud
5. Build Mesh
6. Build Texture
7. Digital elevation model (DEM) + Orthomosaic generation
8. Export DEM and Orthophoto in GeoTIFF format

2.5 Meteorological Data

As an auxiliary information during the geomorphological analysis, I decided to take the information on the wind between the dates of research. Wind rose diagrams have been built from Japan Meteorological Agency (JMA) data. I have used data from closest weather station available—in case of Kujukuri beach it was Mobara (茂原, Table 1) and in case of Uchinada it was Kahoku (かほく, Table 2). Weather station in Kanazawa city is less relevant, because it is located inland, while Kahoku located in coastal area. I used WRE v1.7 (windroseexcel.com) for visualizing information and the Beaufort scale was applied for building diagrams. I abandoned the idea of creating a custom scale so that in the future I would not face need to redo it for another set of data.

Table 1 Sequence of wind data for Kujukuri beach and interrelation with survey time

Survey time	**11-13th of February 2018**	**30th of July 2018**	**15th of September 2018**	**8th of February 2019**
Wind rose time	5 months before 1st survey to compare with 16th of September 2018- 7th of February 2019 period	14th of February – 29th of July 2018	1st of July – 14th of September 2018	16th of September 2018- 7th of February 2019 (approx. 5 month)	---

Table 2 Wind data for Uchinada beach and interrelation with survey time

Survey time	**2nd of September 2018**	**8th of March 2019**
Wind rose time	---	3rd of September 2018- 7th of March 2019	---

3 Results and Analysis

3.1 Point Cloud Properties

A total of 4 surveys were conducted on Kujukuri beach, Chiba Prefecture. As I mentioned previously, first and the rest surveys were conducted in different way, which is reflected in the characteristics.

Table 3 Parameters of each survey on Kujukuri beach

Time	11-13th of February 2018	30th of July 2018	15th of September 2018	8th of February 2019
Camera and UAV	12 mpx, DJI Phantom 3 Standard	12 mpx, DJI Phantom 3 Standard	12 mpx, DJI Phantom 3 Standard	12 mpx, DJI Phantom 3 Standard
Number of Ground Control Points (GCPs) and Check Points (CPs)	39 GCPs and 21 CPs	26 GCPs and 11 CPs	29 GCPs and 11 CPs	26 GCPs and 10 CPs
Number of processed photos	2747	2351	2526	2372
Front&side overlap	80% & 80%	80% & 80%	80% & 80%	80% & 80%
DEM resolution	8.75 cm/px	9.77 cm/px	9.27 cm/px	8.52 cm/px
Total root-mean-square error (RMSe) for checkpoints	3.25 cm	8.9 cm	12.7 cm	13.12 cm
RMSe of longitude	1.5 cm	6.5 cm	9.5 cm	9.4 cm
RMSe of latitude	1.5 cm	3 cm	3.4 cm	5.6 cm
RMSe of altitude	2.4 cm	5.2 cm	7.8 cm	6.5 cm

In case of Uchinada beach 2 surveys were conducted. Due to the remoteness, it was originally decided to lower the requirements for resolution and overall accuracy (RMSe). Although everyone wants to achieve the best accuracy, it does not make sense to achieve centimeter accuracy, when decimeter accuracy is enough for research purposes, especially in large scale. Once again, I would like to recall that the survey with an accuracy of several centimeters conducted on 11-13th of February 2018 were much more time-consuming and laborious. So, a compromise must be sought.

Table 4 Parameters of each survey on Uchinada beach

Time	2nd of September 2018	8th of March 2019
Camera and UAV	12 mpx, DJI Phantom 3 Standard	12 mpx, DJI Phantom 3 Standard
Number of Ground Control Points (GCPs) and Check Points (CPs)	18 GCPs and 8 CPs	18 GCPs and 8 CPs
Number of processed photos	1010	1276
Front&side overlap	80% & 80%	80% & 80%
DEM resolution	16.6 cm/pix	14.9 cm/pix
Total root-mean-square error (RMSe) for checkpoints	13.3 cm	19 cm
RMSe of longitude	5.8	8.9 cm
RMSe of latitude	6.8	6.2 cm
RMSe of altitude	9.9 cm	15.6 cm

3.2 Large Scale High Resolution Coastal Mapping

We obtained digital elevation model (DEM) and orthomosaic for each survey time. Using ArcGIS, I have combined DEM and orthomosaic. DEMs were highlighted, while orthophotos set as semi-transparent. The main goal was to create a simple topographic maps (Figure 4 to Figure 9) where it would be easy to distinguish different morphological zones – primarily beach zone from the dune zone (Figure 3).

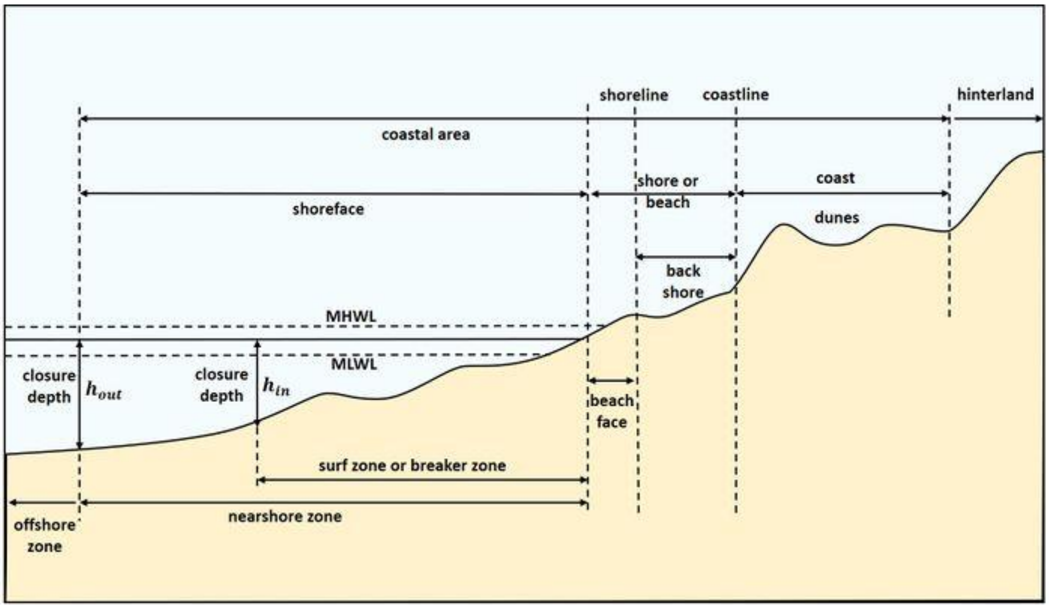

Figure 3 Definition of coastal terms, adapted from Shore Protection Manual (Coastal Engineering Research Center, 1984). Image credit: http://www.coastalwiki.org/wiki/Definitions_of_coastal_terms

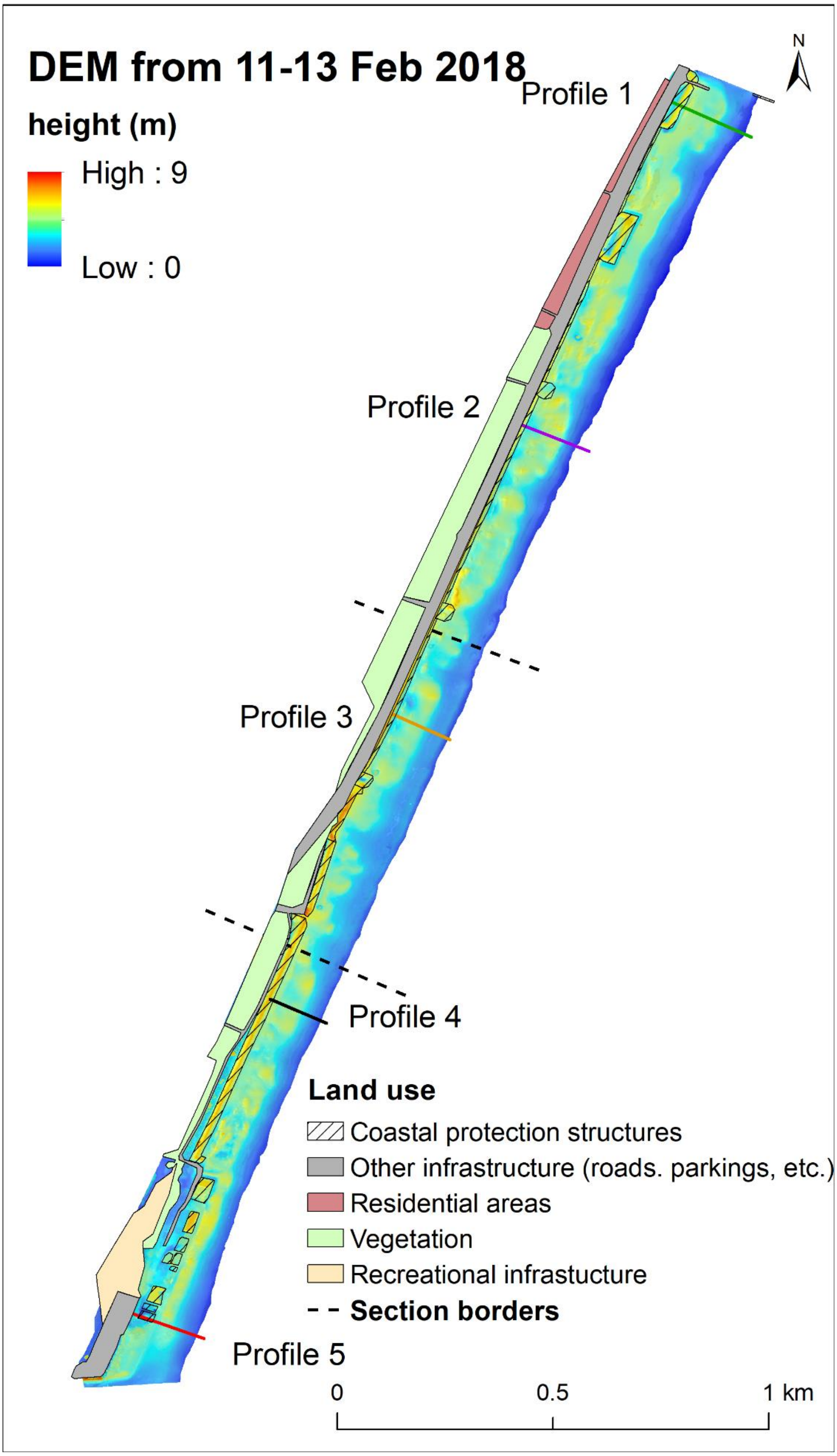

Figure 4 DEM and orthomosaic synthesis of Kujukuri beach during 11-13th of February 2018 survey

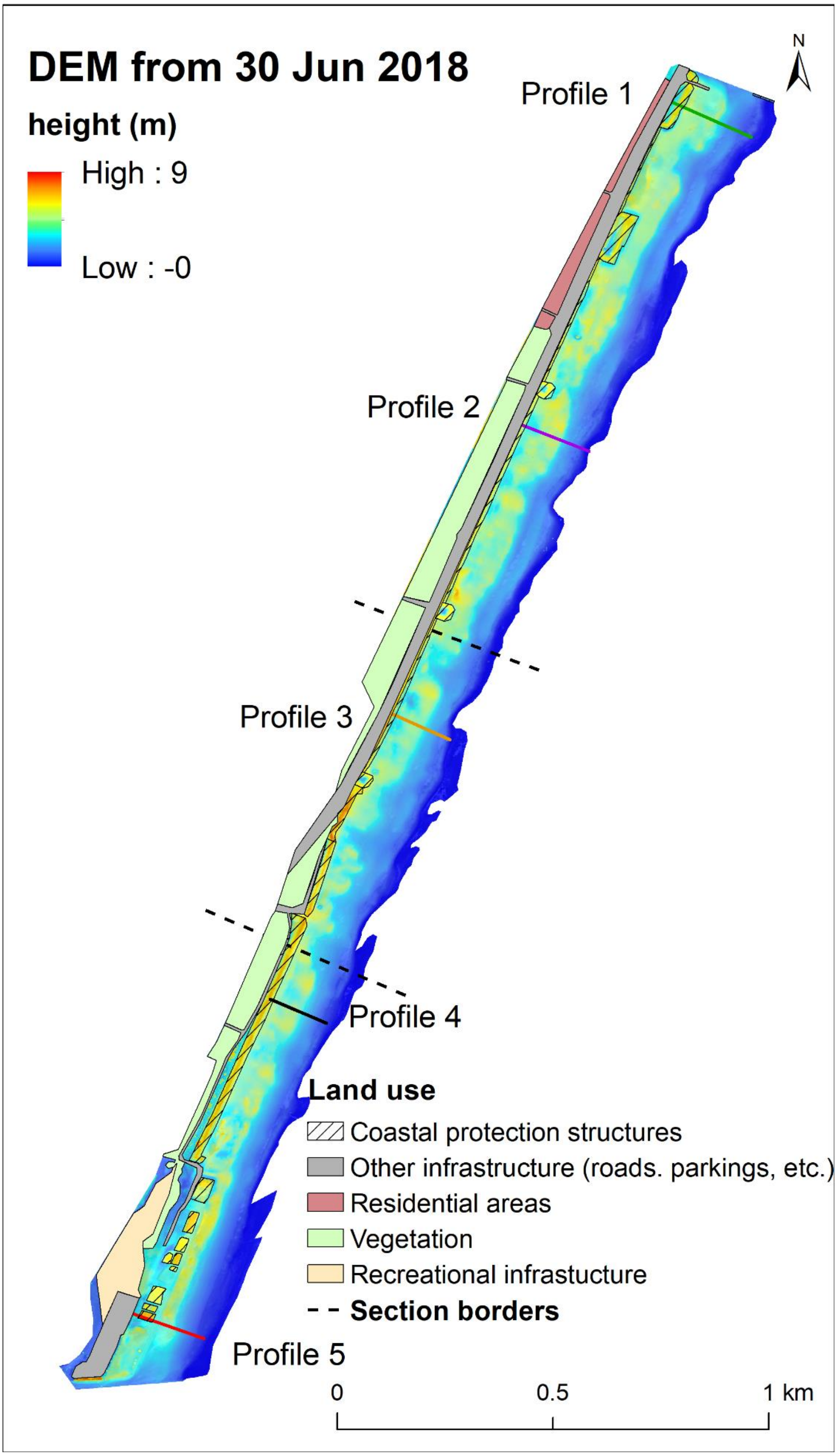

Figure 5 DEM and orthomosaic synthesis of Kujukuri beach during 30th of July 2018 survey

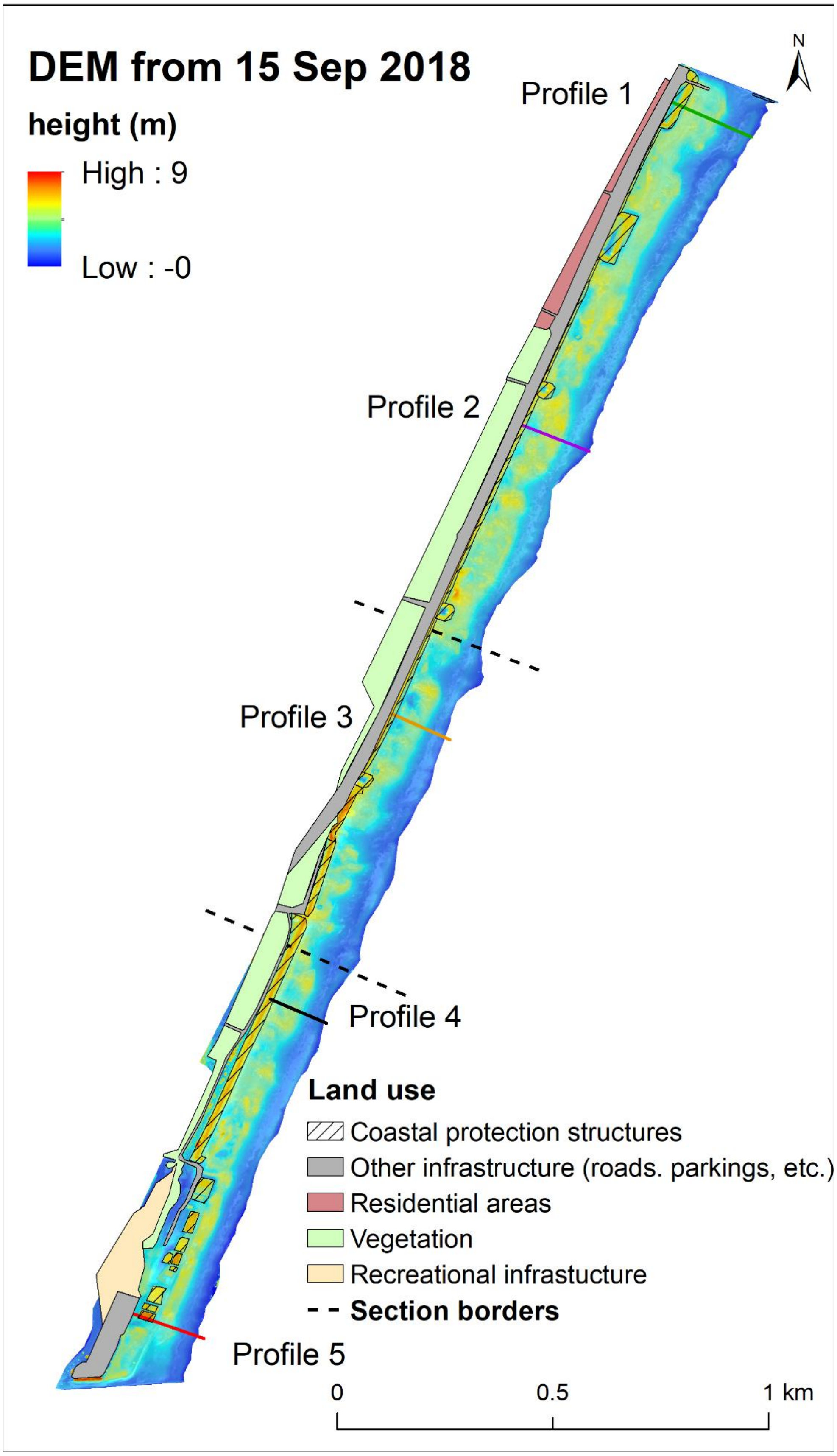

Figure 6 DEM and orthomosaic synthesis of Kujukuri beach during 15th of September 2018 survey

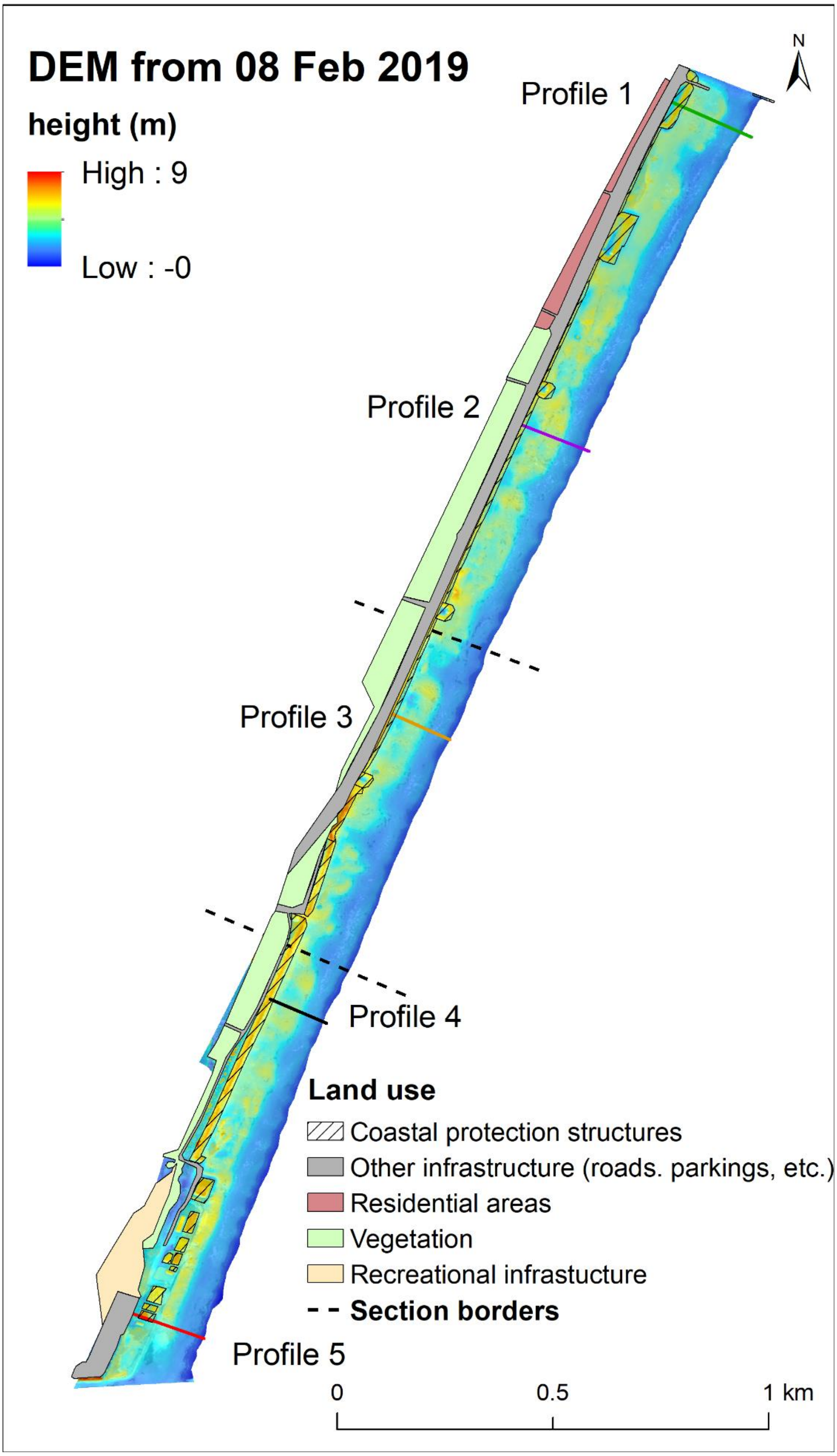

Figure 7 DEM and orthomosaic synthesis of Kujukuri beach during 8th of February 2019 survey

Thanks to the synthesis of DEM and orthomosaic, it became possible to distinguish not only different morphological zones, but also different morphological units. On the Kujukuri beach maps it is very easy to evict evolution of berm. It can be traced as the almost completely eroded berm in February 2018 (Figure 4) is gradually restored in by September 2018 (Figure 6), and then onshore drift happens by February 2019 (Figure 7). In addition, from February to June 2018, it is possible to see how additional coastal protection structures are being built at 2 sites, and at the third, embankments are being prepared.

Unlike Kujukuri, Uchinada beach could not boast developed dune zone (Figure 8). If the northeastern part, even though it is narrow, is still have some distinguishable dunes, then the southeastern part has degraded dune zone. Although there is a slight recovery by spring (Figure 9).

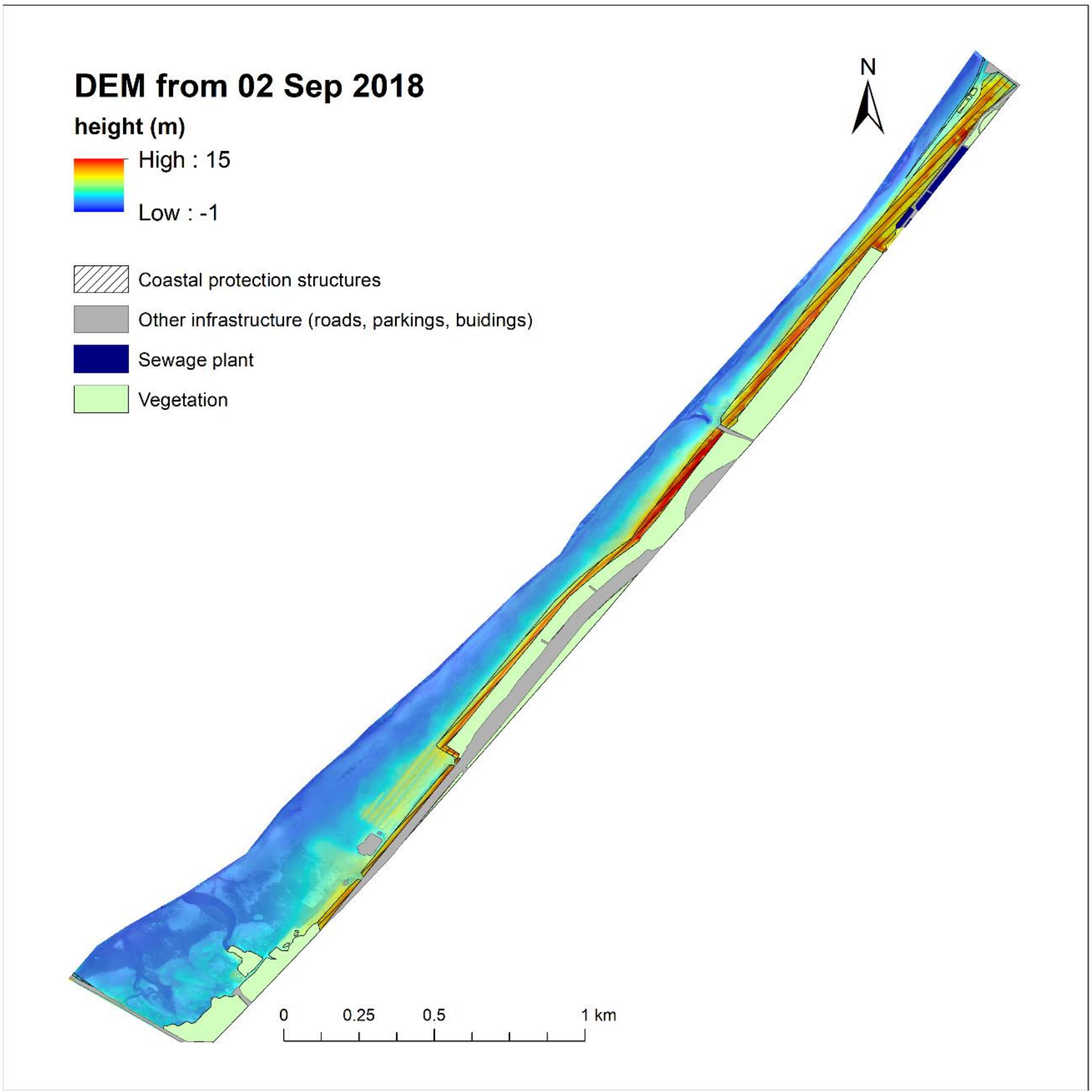

Figure 8 DEM and orthomosaic synthesis of Uchinada beach during 2nd of September 2018 survey

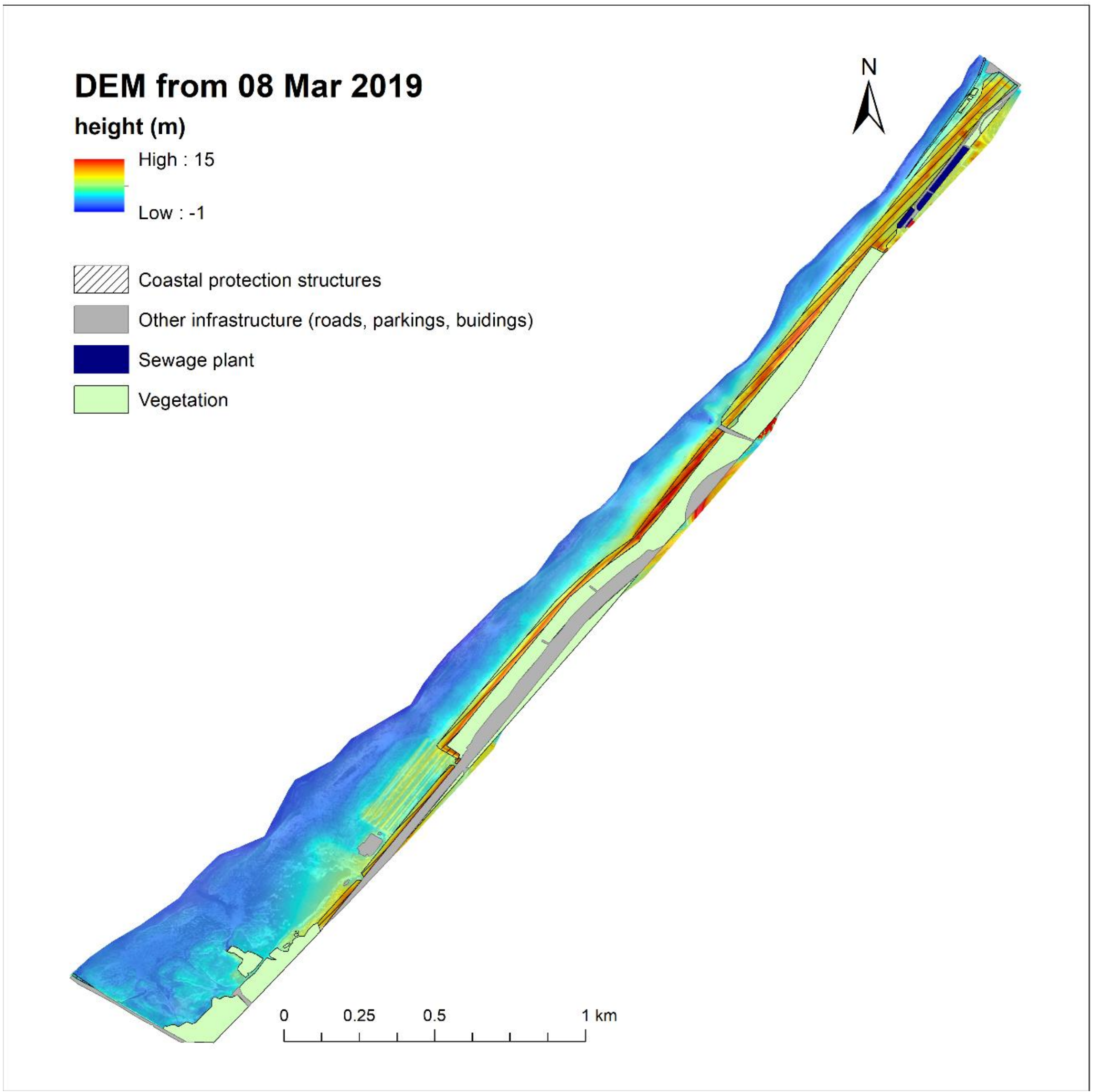

Figure 9 DEM and orthomosaic synthesis of Uchinada beach during 8th of March 2019 survey

3.3 Morphometric Analysis

To achieve greater understanding of beach-dune dynamic I wanted to look at the cross-shore profile. I have used «Profile tool» plugin for QGIS to build 5 cross sectional beach profiles (Figure 10 to Figure 14) with an interval of approximately 750 meters of study area on Kujukuri beach.

Based on both DEM and cross profiles we can assume that northern part of the beach (profile 1 and 2) is different. On both profiles we can see squared foredune crest. Probably it is signs of previous dune erosion. While most active accumulation throughout the year registered in northern section, this section is also subject to dune erosion, so probably northern section is most dynamically active one overall.

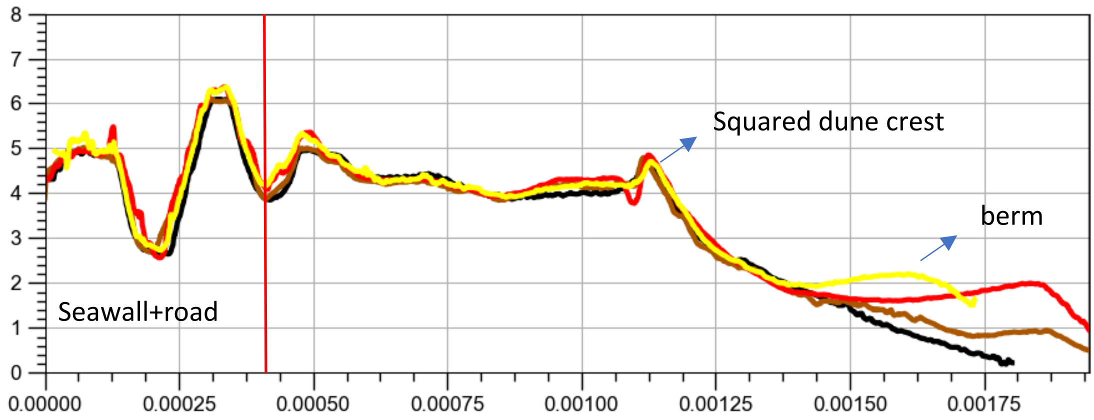

Figure 10 Profile 1 (black line – Feb 2018, brown – June 2018, red – Sep 2018, yellow – Feb 2019)

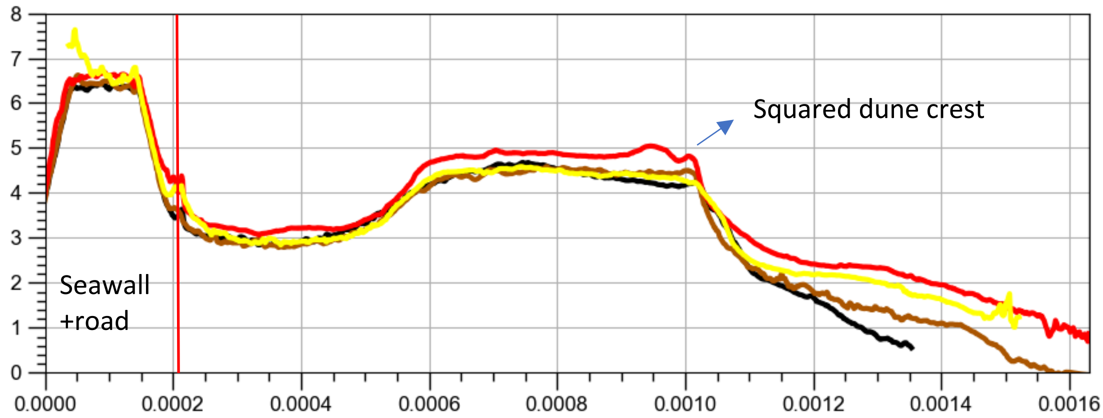

Figure 11 Profile 2 (black line – Feb 2018, brown – June 2018, red – Sep 2018, yellow – Feb 2019)

The central section is the most stable in terms of winter-summer transition. The summer beach profile is maintained throughout the year. Only in June 2018 occurs offshore berm drift, causing erosion only in backshore area.

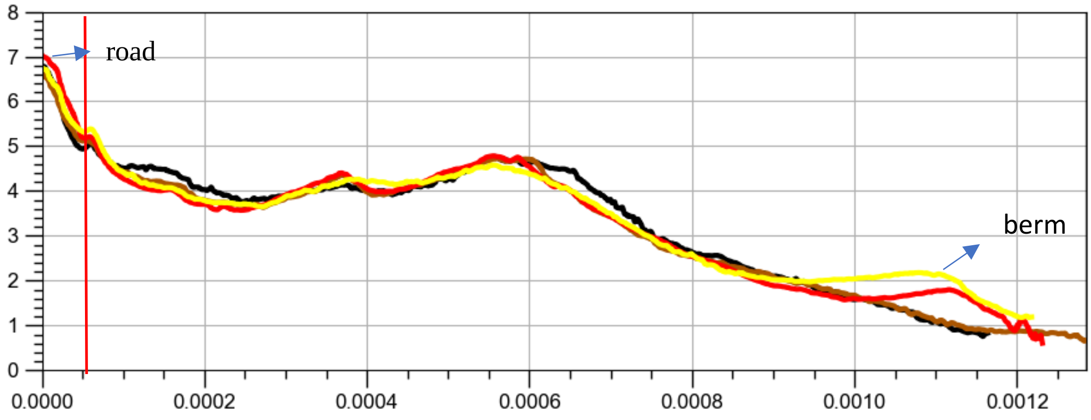

Figure 12 Profile 3 (black line – Feb 2018, brown – June 2018, red – Sep 2018, yellow – Feb 2019)

Both Profiles 4 and 5 are characterized by late transition to summer profile, which happened in mid-summer 2018. Also, unlike the northern section, in southern part the transition from the beach area to the dune area is smoother.

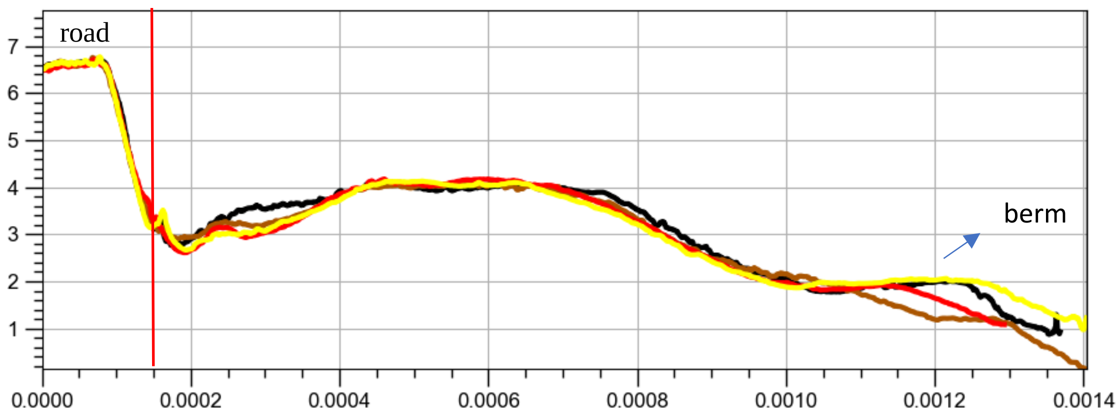

Figure 13 Profile 4 (black line – Feb 2018, brown – June 2018, red – Sep 2018, yellow – Feb 2019)

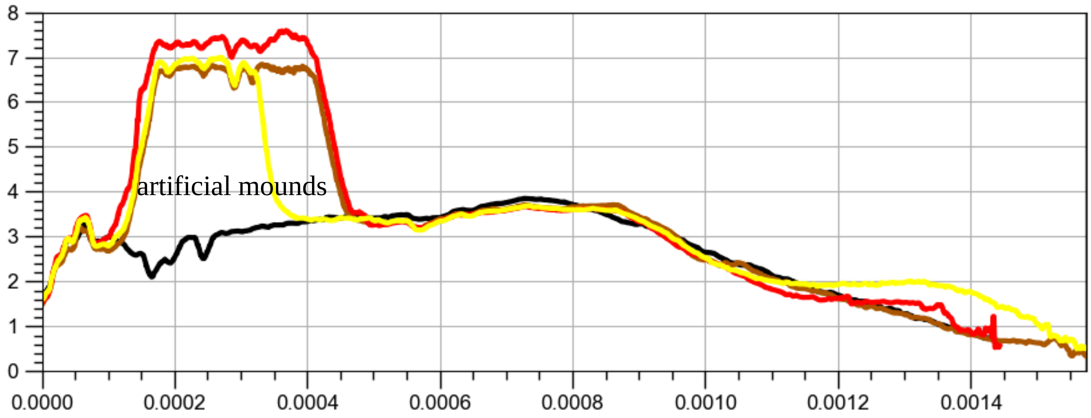

Figure 14 Profile 5 (black line – Feb 2018, brown – June 2018, red – Sep 2018, yellow – Feb 2019)

If we bring summer-winter transition dynamic for each profile into one table (Table 5), we can clearly distinguish 3 separate sections with different dynamics. Northern section characterized by most active accumulation and fast transition from winter beach to summer. The central section is the most stable in terms of winter-summer transition. In southern section, unlike in northern, transition from winter beach to summer happens with a delay.

Table 5 Winter-summer dynamic for each profile

	Profile 1	**Profile 2**	**Profile 3**	**Profile 4**	**Profile 5**
Feb 2018	Winter beach	Winter beach	Summer beach	Winter beach	Winter beach
Jun 2018	Summer beach	Summer beach	Summer beach	Winter beach	Winter beach
Sep 2018	Summer beach	Summer beach	Summer beach	Summer beach	Summer beach
Feb 2019	Summer beach	Summer beach	Summer beach	Summer beach	Summer beach
	Northern section		Central section	Southern section	

3.4 Analysis of Topographical Changes based on Meteorological Data

In addition to spatial data it was important to add some sort of meteorological data. In most cases, researchers rely on the wind data, because acquiring wave data most of the times impossible or quite expensive. So, we have built wind rose diagrams based on data derived from Japan Meteorological Agency (JMA) data. In case of Kujukuri beach, I have used data from closest weather station available—Mobara (茂原). The Beaufort scale was applied to build diagrams. As you can see (Figure 16), from Feb to June 2018 alongshore winds prevailed, mostly SSW and NNE.

From Feb 2018 to Jun 2018 we can observe only partial transition from winter profile to summer (Figure 15).

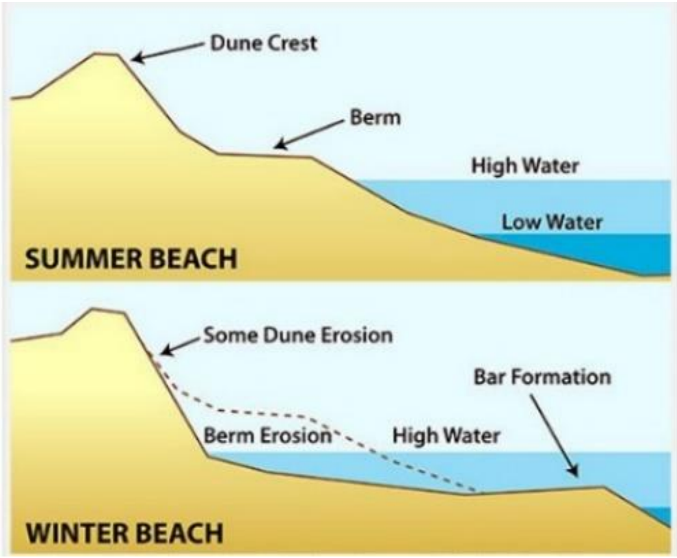

Figure 15 Illustration of winter and summer profile
(image credit: https://www.friendsofibsp.org/breaking-news/science-of-the-shore-a-tale-of-two-beaches-winter-summer-beach-profiles/)

To analyze topography, I uploaded digital elevation models to ESRI ArcGIS. Using the raster calculator from 3D Analyst I was able to measure difference in altitude between each survey time. Beach accumulation (red areas) and formation of the berm occurs only in the northern part, and in the central part even beach erosion (blue areas) is observed (Figure 16).

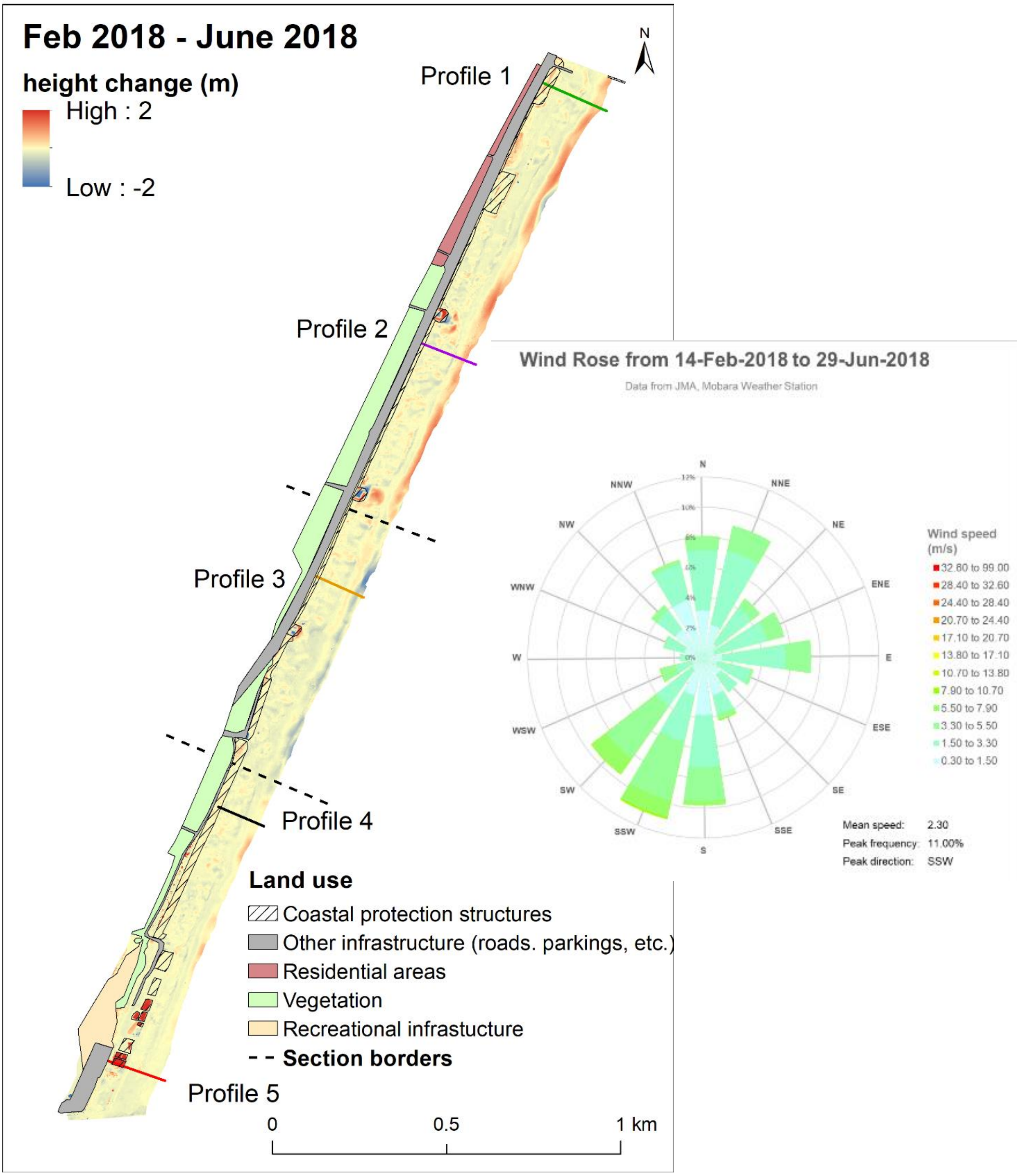

Figure 16 Topographic changes on Kujukuri beach from Feb 2018 to Jun 2018 (left) and wind rose for Mobara weather station from 14th of Feb to 29th of Jun 2018 (right)

In 2018 between beginning of July and mid-September the nature of the wind changes slightly (Figure 17), becoming mainly alongshore.

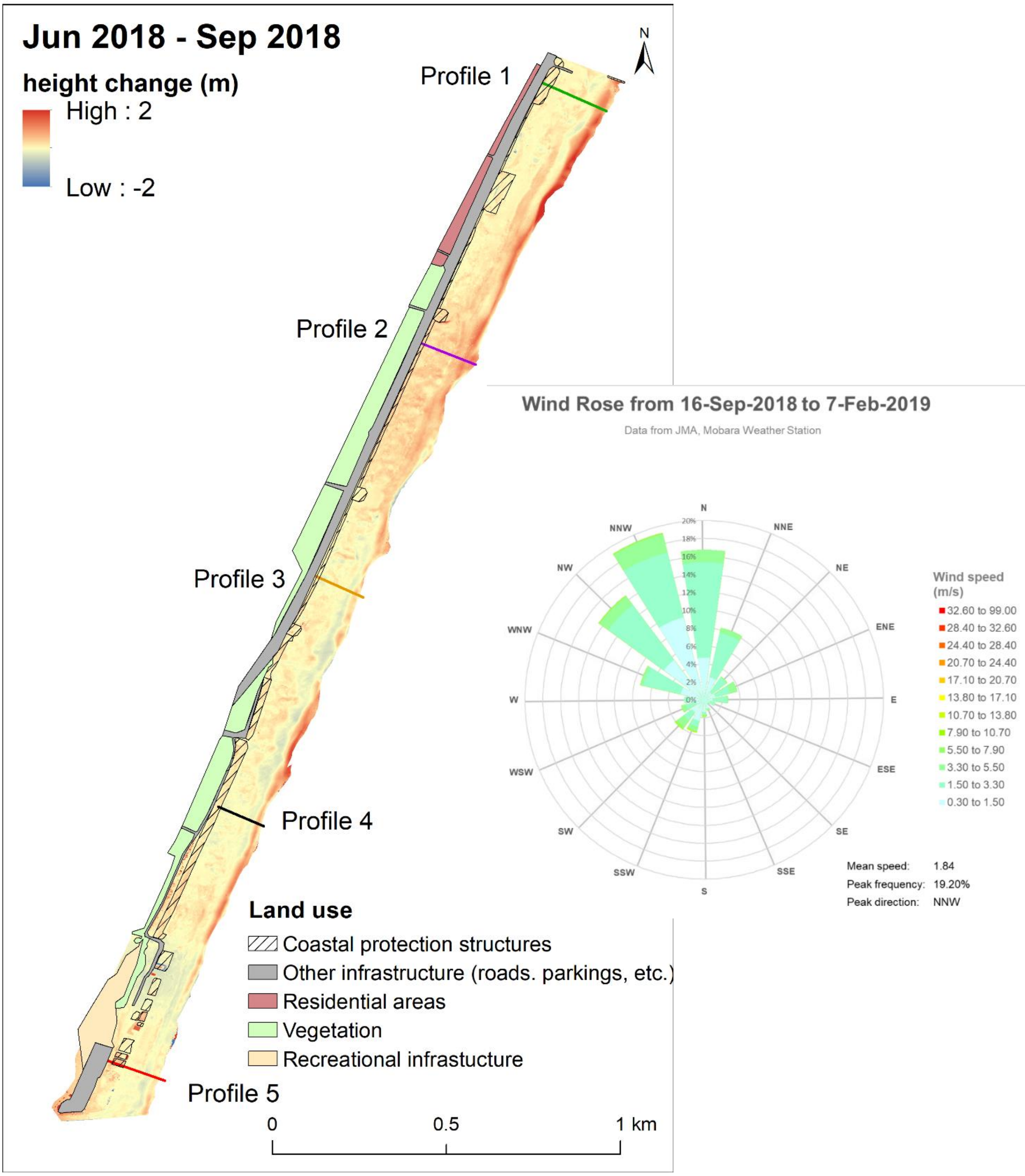

Figure 17 Topographic changes on Kujukuri beach (left) and wind rose for Mobara weather station (right) from 1st of July to 14th of Sep 2018 period

From Feb 2018 to Sep 2018 we can observe a complete transition from winter profile to summer. In 2018, summer profile is set between beginning of July and mid-September. Prevailing winds (SW and SSW) are similar with previous survey gap, so seems like SW and SSW winds drive accumulation.

We assumed that in February 2019 winter profile will set again (Figure 18).

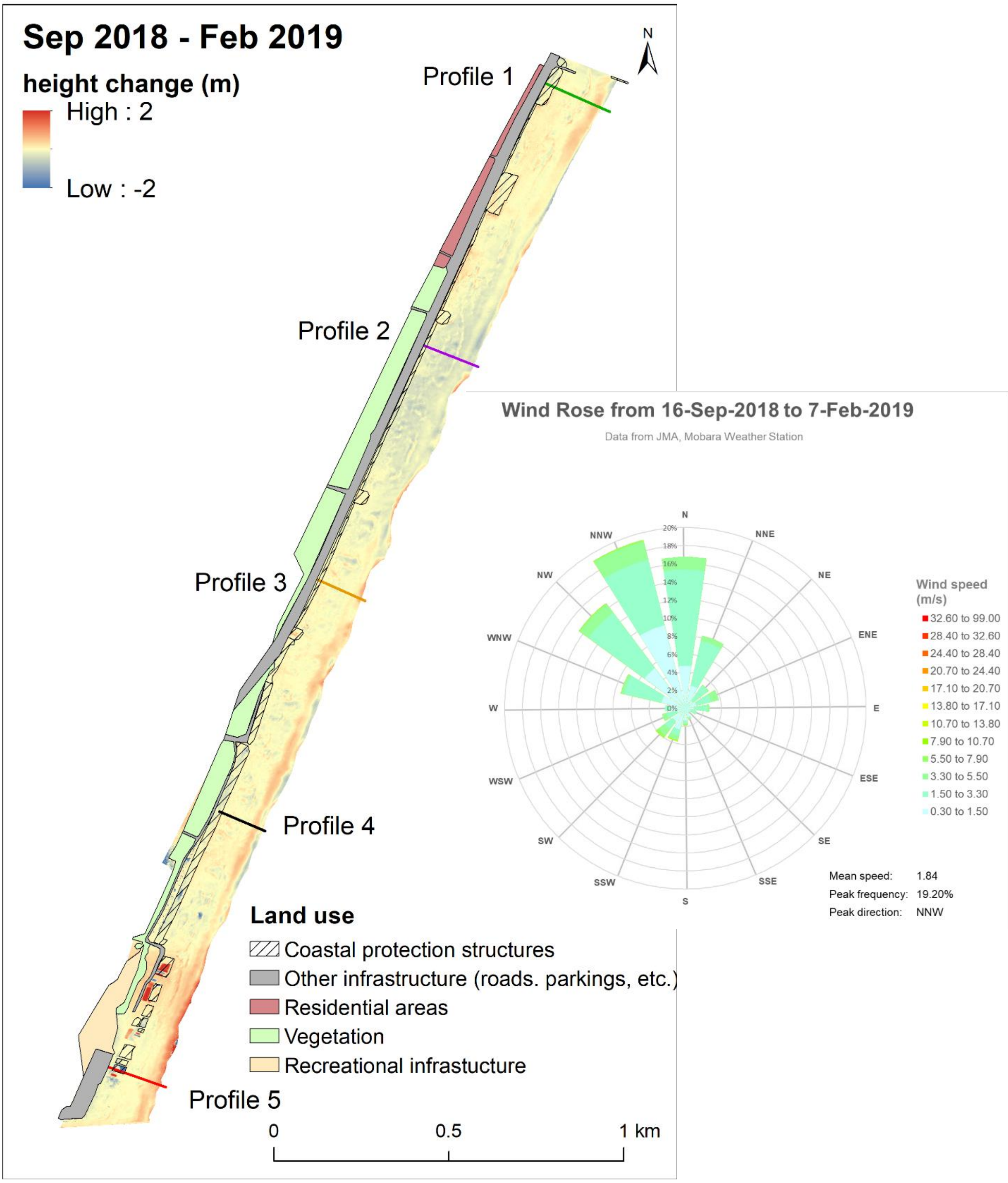

Figure 18 Topographic changes on Kujukuri beach (left) and wind rose for Mobara weather station (right) from 16th of Sep 2018 to 7th of Feb 2019

But from Sep 2018 to Feb 2019 we still observe accumulation, but mostly in backshore area. While foreshore erosion can be observed in some areas. It happens because of onshore berm drift. Seem like onshore drift happens because of prevailing onshore winds during autumn-winter season.

So, in Feb 2019 we still observe summer profile, there was not any berm erosion during autumn-winter. To understand why this happens we built wind rose for the interval of 5 month before our 1st survey, similar to interval between 3rd and 4th surveys.

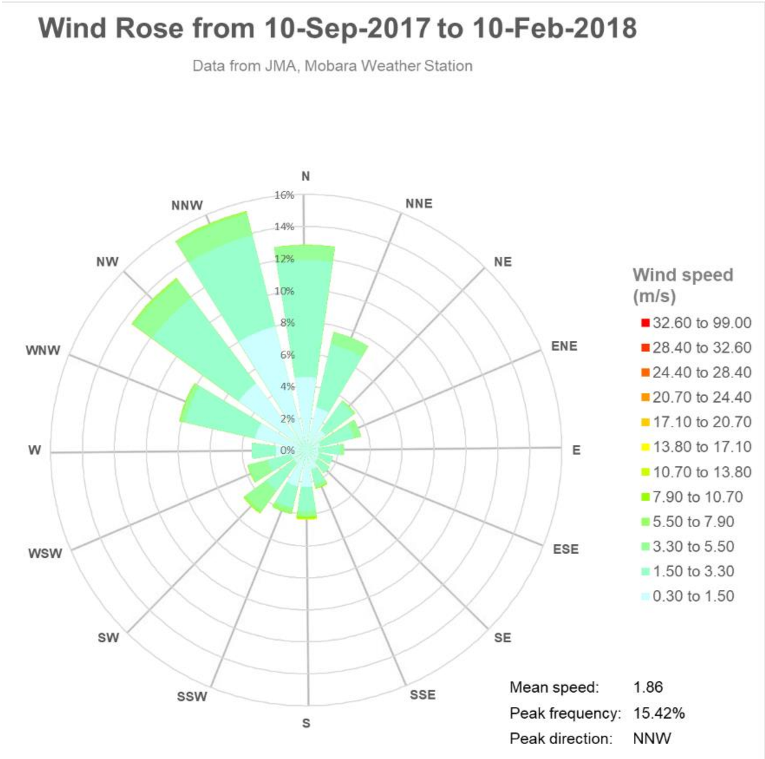

Figure 19 Wind rose for Mobara weather station from 10th of Sep 2017 to 10th of Feb 2018

Prevailing winds for autumn-winter 2018-2019 season (Figure 18) is quite similar to winds during autumn-winter 2017-2018 (Figure 19). Both mean speed and peak direction are similar. So, I would assume that seasonal shift from winter profile to summer profile and vice versa happens during specific storm events rather than wind regime change.

As a result of absence such kind of specific storm event - active accumulation is observed on the beach throughout the year from Feb 2018 to Feb 2019 (Figure 20), especially in the backshore area.

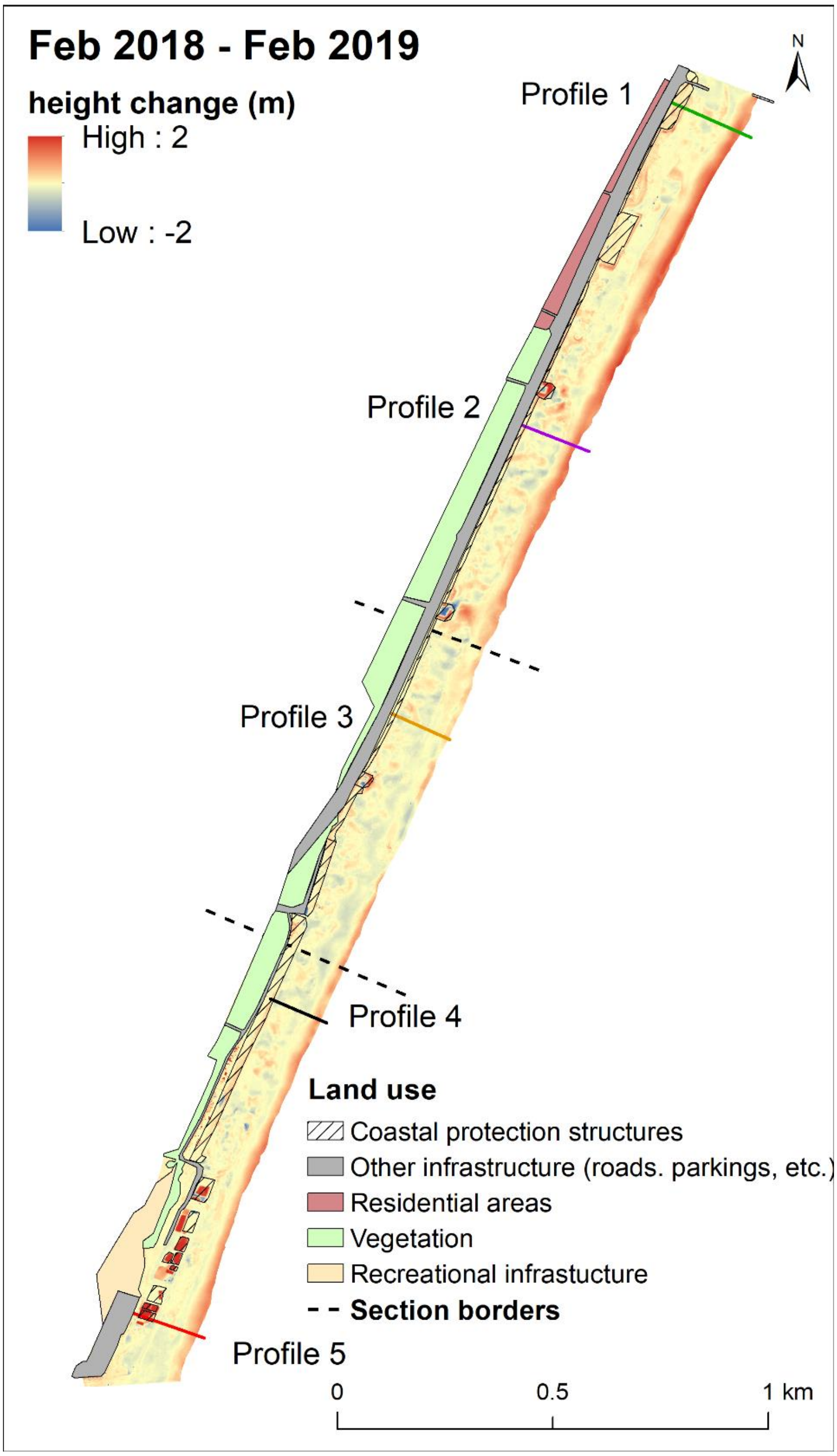

Figure 20 Total topographic change on Kujukuri beach from February 2018 to February 2019

The nature of the wind rose in case Uchinada beach (Figure 21) is different because of the location of weather station. Unlike Mobara station in case of Kujukuri beach, Kahoku Station is located on the coast, so you can clearly distinguish sea and land breezes. Land breezes happens to be less frequent, but stronger.

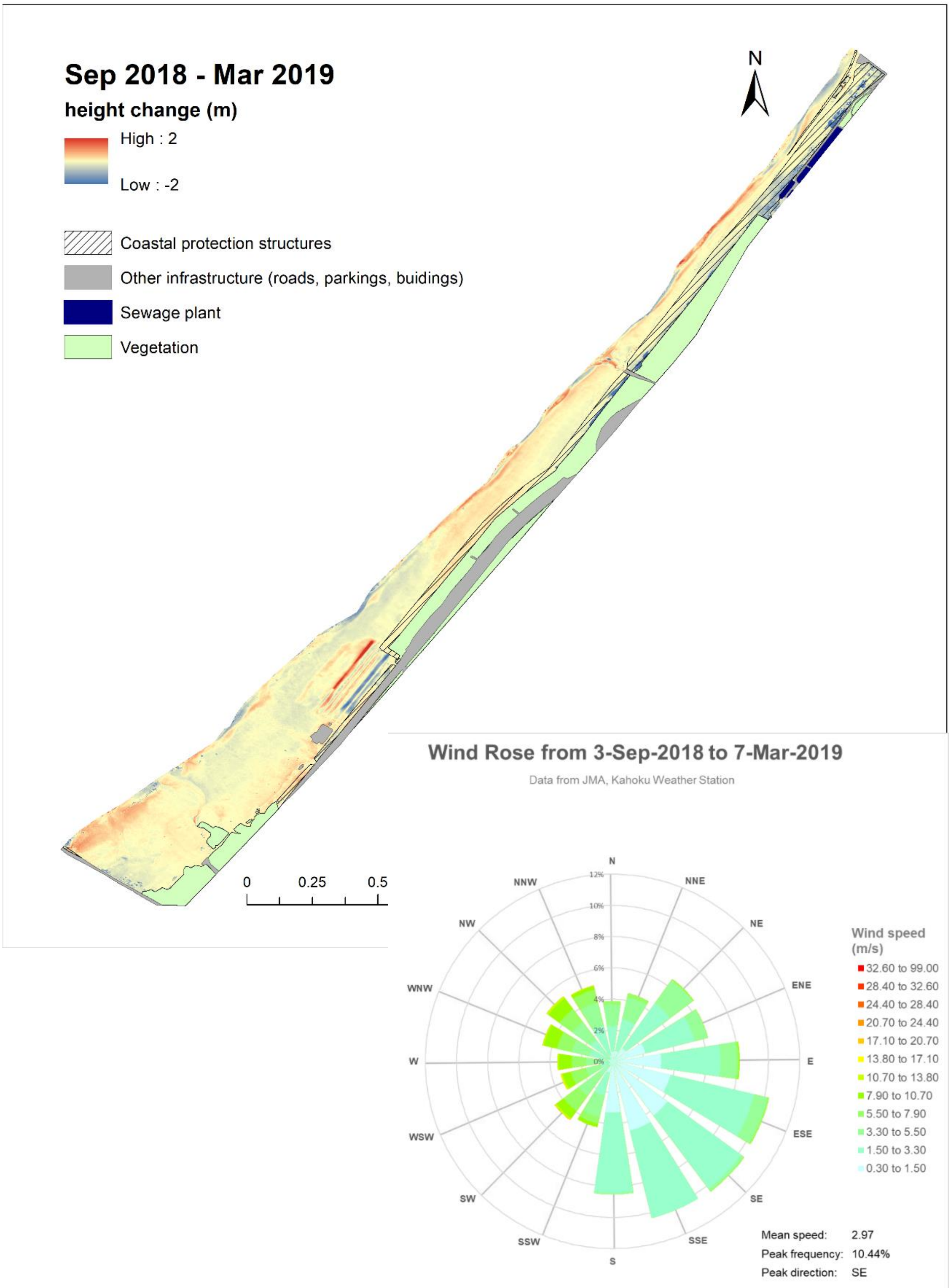

Figure 21 Topographic changes on Kujukuri beach (up) and wind rose for Kahoku weather station (down) from 3rd of Sep to 7th of Mar 2019

3.5 Comparison Between Kujukuri and Uchinada Beaches

As I mentioned before, unlike Kujukuri, Uchinada beach could not boast developed dune and beach zones. During summertime is under heavy influence of human activity. People use vehicle to travel along the beach, causing degradation of the beach. With the onset of winter human activity reduces, so the beach starts to restore back to natural processes.

In general, both Uchinada and Kujukuri beaches depend on sediments coming from offshore. The only difference is that due to the human impact the active accumulation phase on Uchinada beach happens during autumn-winter season depends on sediments coming from underwater coastal slope.

It turns out that the difference between the beaches is caused not only by different natural conditions, but mainly by the difference in approaches to the coastal management of various municipalities. This demonstrates the importance of human impact assessment and proper coastal management.

4 Discussion

4.1 Overall Benefits and Limitations of UAV SfM

So, even low-cost UAV SfM gives us great insight into beach-dune dynamics across large area at high resolution. If you look at the classification of various coastal monitoring methods by scale, created by Sutherland in 2007 (Sutherland, 2007):

1. Small scale – linear arrays of point sensors, underwater acoustic measurements of the seabed, measurements of emerged toe levels, measurements of mixing depth;
2. Medium scale – cross shore profile surveys and topographic surveys, total station, kinematic GPS, laser scanning systems, CRAB&WESP, repeated digital photography, x-band radar;
3. Large scale – map tidelines and shorelines, orthorectified aerial or satellite photos, topographic lidar, bathymetric lidar, bathymetric surveying;

You will find out that different methods have different disadvantages. For example, some of them simply requires very expensive tools (topographic lidar, total station), the second have a limited scale (practically all from point 1 and 2), the third provide discontinuous spatial data and when you try to fix this flaw they become extremely laborious (cross-shore profile surveys and topographic surveys), fourth do not give full control over the parameters of the study and you have rely on a third party (orthorectified aerial or satellite photos). While UAV SfM is not perfect - for example, it does not provide any bathymetry data - it gives you continuous spatial data with less effort practically wherever and whenever you want with controlled scale and high resolution. It is not surprising that it gained such popularity in a short time.

On the other hand, high resolution gives us an understanding that the seemingly trivial human impact can cause huge degradation of coastal processes. At the same time, high resolution in combination with increasing scale and sequence of monitoring can lead to the increased processing and analyzing complexity. The next logical step would be automatization of some analysis using deep-learning (Buscombe & Ritchie, 2018), automatic feature extraction and object-based image analysis (Papakonstantinou, Topouzelis, & Pavlogeorgatos, 2016)& (Sturdivant, et al., 2017).

4.2 Human Impact Assessment

On Kujukuri beach we were able to capture controlled human activity - construction of coastal protection structures, implementation of the governmental program after 2011 Tōhoku earthquake and tsunami. While we were able to capture only construction of additional structures, we still managed to fix the changes in the morphology of dune zone. Impact is rather local and limited, but the overall monitoring time is still insufficient to draw long-term conclusions.

On Uchinada beach during first survey we witnessed high level of uncontrolled human activity. Especially human impact was obvious on the southeast of the Uchinada beach. While, I previously mentioned that with the onset of winter human activity reduces, during our second survey we still witnessed relatively high human activity. This is especially noticeable in contrast with the situation on the Kujukuri beach. Herewith UAV SfM could reveal to us the scale of the problem and the ability of beach-dune system to restore.

5 Conclusion

Kujukuri beach

- From Feb 2018 to Sep 2018 we can observe an overall transition from winter profile to summer. In 2018, summer profile is set between beginning of July and mid-September.
- It was assumed that in February 2019 winter profile will settle again. But in Feb 2019 we still observe summer profile.
- At the same time, the wind data for autumn-winter 2018-2019 is not different from the data for autumn-winter 2017-2018. Both mean speed and peak direction are quite similar.
- As a result, active accumulation is observed on the beach throughout the year, especially in the backshore area.
- In contrast to the autumn-winter season, during the spring-summer season the prevailing winds are the alongshore winds. During this period active accumulation happens and formation of the summer profile occurs.
- Based on both DEM and cross profiles we can differentiate 3 sections with separate dynamic.
- Northern section characterized by most active accumulation and fast transition from winter beach to summer. The central section is the most stable in terms of winter-summer transition. In southern section, unlike in northern, transition from winter beach to summer happens with a delay.
- Controlled human activity on Kujukuri beach (construction of coastal protection structures) have a rather local and limited effect on natural processes.

Uchinada beach

- Unlike Kujukuri beach, Uchinada beach during summertime is under heavy influence of uncontrolled human activity. People use vehicle to travel along the beach, causing degradation.
- With the onset of winter human activity reduces, so the beach starts to restore back to natural processes.
- Most active accumulation (up to 1.2-1.5 meters) happens on the beach. Largest area of beach accumulation is in the southern part of study area, which is under highest influence of human activity due to accessibility by vehicles. Also, there is long area of beach accumulation in the central part of study area.
- Although not universally, there are large areas of accumulation in the dune zone.
- Seems like, in general, Uchinada beach during autumn-winter season depends on sediments coming from offshore, allowing the beach to regenerate.

Discreteness of coastal processes lead to uneven coastal dynamics within single morpho- and lithological unit. Overall, increasing scale of UAV SfM survey gives us broader view of beach-dune dynamics, while decreasing researcher bias.

Combination of meteorological data and geomorphological data gave us an understanding that seasonal changes in coastal geomorphology can be caused not only by seasonal weather variations as it would seem at first glance, but by specific weather conditions, such as storms and typhoons.

High resolution gives us an understanding that the seemingly trivial human impact can cause huge degradation of coastal processes.

High resolution in combination with increasing scale and sequence of monitoring can lead to the increased processing and analyzing complexity. The next logical step would be automatization of some analysis using deep-learning, automatic feature extraction and object-based image analysis.

6 References

Boon, M. A., Drijfhout, A. P., & Tesfamichael, S. (2017). Comparison of a Fixed-Wing and Multi-Rotor Uav for Environmental Mapping Applications: A Case Study. *The International Archives of Photogrammetry, Remote Sensing and Spatial Information Sciences, 42*, 47.

Buscombe, D., & Ritchie, A. (2018). Landscape classification with deep neural networks. *Geosciences, 8(7)*, 244.

Carbonneau, P. E., & Dietrich, J. T. (2017). Cost-effective non-metric photogrammetry from consumer-grade sUAS: implications for direct georeferencing of structure from motion photogrammetry. *Earth Surface Processes and Landforms, 42(3)*, 473-486.

Casella, E., Rovere, A., Pedroncini, A., Stark, C. P., Casella, M., Ferrari, M., & Firpo, M. (2016). Drones as tools for monitoring beach topography changes in the Ligurian Sea (NW Mediterranean). *Geo-Marine Letters, 36(2)*, 151-163.

Coastal Engineering Research Center. (1984). *Shore protection manual.* Department of the Army, Waterways Experiment Station.

Erikkson, S. (2016). *Real-time kinematic positioning of UAS-possibilities and restrictions.* (Doctoral dissertation, Tesis de Maestrıa, Chalmers University of Technology).

Laporte-Fauret, Q., Marieu, V., Castelle, B., Michalet, R., Bujan, S., & Rosebery, D. (2019). Low-Cost UAV for high-resolution and large-scale coastal dune change monitoring using photogrammetry. *Journal of Marine Science and Engineering, 7(3)*, 63.

Mancini, F., Dubbini, M., Gattelli, M., Stecchi, F., Fabbri, S., & Gabbianelli, G. (2013). Using unmanned aerial vehicles (UAV) for high-resolution reconstruction of topography: The structure from motion approach on coastal environments. *Remote Sensing, 5(12)*, 6880-6898.

Medjkane, M., Maquaire, O., Costa, S., Roulland, T., Letortu, P., Fauchard, C., & Davidson, R. (2018). High-resolution monitoring of complex coastal morphology changes: cross-efficiency of SfM and TLS-based survey (Vaches-Noires cliffs, Normandy, France). *Landslides, 15(6)*, 1097-1108.

Oniga, V. E., Breaban, A. I., & Statescu, F. (2018). Determining the optimum number of ground control points for obtaining high precision results based on UAS images. *Multidisciplinary Digital Publishing Institute Proceedings, Vol. 2, No. 7,* (p. 352).

Papakonstantinou, A., Topouzelis, K., & Pavlogeorgatos, G. (2016). Coastline zones identification and 3D coastal mapping using UAV spatial data. *ISPRS International Journal of Geo-Information, 5(6)*, 75.

Robustelli, U., Baiocchi, V., & Pugliano, G. (2019). Assessment of dual frequency GNSS observations from a Xiaomi Mi 8 Android smartphone and positioning performance analysis. *Electronics, 8(1)*, 91.

Sturdivant, E., Lentz, E., Thieler, E. R., F. A., Weber, K., Remsen, D., & Henderson, R. (2017). UAS-SfM for coastal research: Geomorphic feature extraction and land cover classification from high-resolution elevation and optical imagery. *Remote Sensing, 9(10),* 1020.

Sutherland, J. (2007). Inventory of coastal monitoring methods and overview of predictive models for coastal evolution. *CONSCIENCE Deliverable Report D, 1*.

Tamura, T., Murakami, F., & Watanabe, K. (2010). Holocene beach deposits for assessing coastal uplift of the northeastern Boso Peninsula, Pacific coast of Japan. *Quaternary Research, 74(2),* 227-234.

Tonkin, T., & Midgley, N. (2016). Ground-control networks for image based surface reconstruction: An investigation of optimum survey designs using UAV derived imagery and structure-from-motion photogrammetry. *Remote Sensing, 8(9),* 786.

Vacca, G., Dessì, A., & Sacco, A. (2017). The use of nadir and oblique UAV images for building knowledge. *ISPRS International Journal of Geo-Information, 6(12),* 393.

Westoby, M. J., Lim, M., Hogg, M., Pound, M. J., Dunlop, L., & & Woodward, J. (2018). Cost-effective erosion monitoring of coastal cliffs. *Coastal Engineering, 138*, 152-164.

7 Acknowledgment

Foremost, I would like to express gratitude to my research adviser Prof. Sugai for the endless support and guidance during this scientific journey. Your vast knowledge and expertise became the foundation of this study. I could not ask for better adviser than you.

Further, I want to heartily thank Dr. Natsuki Sasaki and Dr. Shoichiro Uchiyama. Your help and expertise were indispensable. You were a guiding light for me.

I also thank my colleagues from laboratory of Natural Environmental Changes who helped during my countless field surveys: Taiga Kimori, Tatsuki Miyamoto, Atsuto Izumida, as well as, Taro Funatsu from Department of Earth and Planetary Science.